PHYSICAL REVIEW B **76**, 220506(R) (2007)

Local superfluid densities probed via current-induced superconducting phase gradients

David S. Hopkins, David Pekker, Tzu-Chieh Wei, Paul M. Goldbart, and Alexey Bezryadin
Department of Physics and Frederick Seitz Materials Research Laboratory, University of Illinois at Urbana-Champaign, Urbana, Illinois 61801, USA

(Received 26 September 2007; published 13 December 2007)

We have developed a superconducting phase gradiometer consisting of two parallel DNA-templated nanowires connecting two thin-film leads. We have ramped the cross current flowing perpendicular to the nanowires, and observed oscillations in the lead-to-lead resistance due to cross-current-induced phase differences. By using this gradiometer we have measured the temperature- and magnetic-field dependence of the superfluid density, and observed an amplification of phase gradients caused by elastic vortex displacements. We examine our data in light of Miller-Bardeen theory of dirty superconductors and a microscale version of Campbell's model of field penetration.

DOI: 10.1103/PhysRevB.76.220506 PACS number(s): 74.50.+r, 74.78.−w

Gradients in the phase of the superconducting order parameter can be generated by external magnetic fields and sensed using a superconducting quantum interference device (SQUID), invented by Jaklevic *et al.*[1] Applications of SQUIDs are numerous.[2] As demonstrated by Clarke and others, SQUIDs may be used as magnetometers to detect remarkably small magnetic fields, e.g., magnetic fields occurring in living organisms.[3] A voltmeter based on the SQUID, also developed by Clarke, is capable of measuring 10 fV, i.e., it is 10^5 times more sensitive than a conventional semiconductor voltmeter.[4] Microscale and nanoscale realizations of SQUIDs have been fabricated, e.g., in shunted Nb nanojunctions having a submicron hole[5] and, more recently, using nanotubes.[6] SQUIDs have also been used to study macroscopic quantum phenomena and devices, such as magnetization tunneling[7,8] and phase qubits.[9]

In this paper we report on a version of the Jaklevic *et al.* phase-sensing experiment, in which DNA-templated superconducting nanowires are used instead of Josephson junctions to make a nanowire version of a SQUID (i.e., an *N*-SQUID). Our main accomplishments are as follows. (1) By measuring the period of the resistance oscillations driven by an externally injected supercurrent, we have performed a direct, local measurement of the superfluid density and its dependence on temperature in the vortex-free regime. Our results are inconsistent with the phenomenological Gorter-Casimir and Ginzburg-Landau models, but are in good agreement with the Miller-Bardeen (MB) dirty limit of the microscopic BCS theory,[10] which was previously examined for MoGe via a different method by the Lemberger group.[11] (2) We have observed and investigated the amplification of the current-induced phase gradient that occurs when pinned vortices are present in the cross-current-carrying lead. This amplification is brought about by a Lorentz force, which acts on randomly pinned vortices and results in their reversible displacement. In macroscopic settings, this physical phenomenon is the origin of the Campbell law, i.e., the dependence of the magnetic-field penetration depth on the concentration of vortices.[12–15] Our measurements provide a verification of the physics behind the Campbell law, but now at the microscale, as well as the capability of obtaining the Labusch parameter, i.e., the average stiffness of the vortex pinning potential.

The fabrication of our device begins by following the steps described in Ref. 16. First, a pair of DNA molecules are suspended across a trench etched into SiN/SiO_2 on a Si chip. Second, the molecules and the banks are sputter-coated with $Mo_{79}Ge_{21}$ to create a pair of parallel superconducting nanowires that join two superconducting leads. Finally, the basic shape of the leads is defined via optical lithography. Next, we perform an additional step, in which a focused ion beam (FIB) is used to cut one of the leads into a horseshoe shape, and thus define a narrow strip through which a cross current (I_X) can be applied (see Fig. 1). Independently, a bias current (I_B) can be applied through the nanowires, via which the lead-to-lead resistance can be measured.[17] The typical width of the cross-current strip is of the order of $w=700$ nm (e.g., 633 nm for sample No. 2), which is much smaller than the zero-temperature perpendicular penetration depth $\lambda_\perp=46$ μm. Thus, the analysis of the results will be carried out under the assumption that I_X flows uniformly in the cross-current strip. The width of the larger of the two leads $2l=17.33$ μm is also smaller than $\lambda_\perp$, and thus any external field will penetrate both leads without significant attenuation. Moreover, we estimate that the effects of the Ampère magnetic field generated by the cross current are negligible. The length of the nanowires, denoted by b, is 100 nm for sample No. 2, and the distance between them, denoted by $2a$, which determines the spatial resolution of the device, is 3.13 μm for this sample. Deviceswith better spatial resolution (e.g., with $2a\sim265$ nm) were demonstrated in a different setup.[16]

At $I_X=0$, we observe a broad resistive transition in the nanowires, as the temperature T is decreased. Moreover, as I_X is increased, this transition periodically broadens and nar-

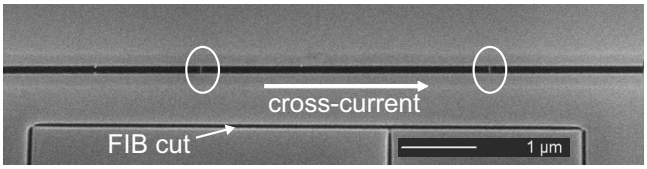

FIG. 1. SEM micrograph of the device. The trench separating the leads is the dark feature running horizontally across the micrograph and the two nanowires (circled) can be seen crossing the trench. The FIB cut and the cross-current direction are indicated.

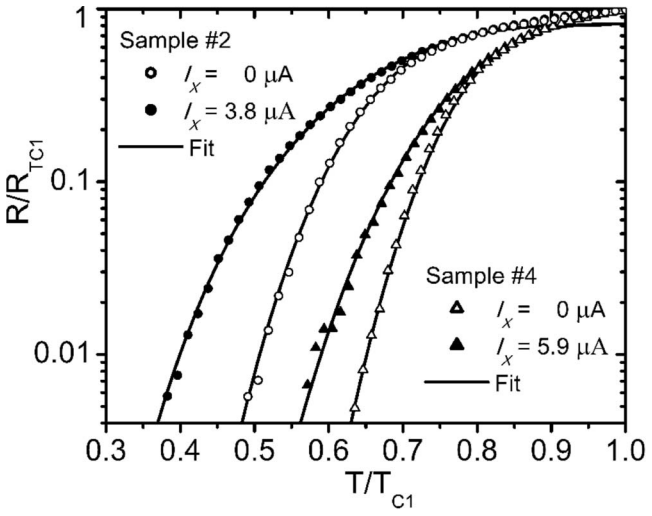

FIG. 2. Resistance vs temperature data for samples No. 2 (circles) and No. 4 (triangles). The open shapes correspond to zero cross-current measurements and the filled shapes correspond to a cross current that gives a resistance close to a maximum (3.8 μA for sample No. 2 and 5.9 μA for sample No. 4). The fits are obtained with the following fit-parameters: sample No. 2–R_N=800 Ω, $I_{c1}(0)$=376 nA, $I_{c2}(0)$=151 nA, T_{c1}=2.45 K, T_{c2}=1.86 K and sample No. 4–R_N=700 Ω, $I_{c1}(0)$=1066 nA, $I_{c2}(0)$=317 nA, T_{c1}=3.04 K, T_{c2}=2.55 K (Ref. 26).

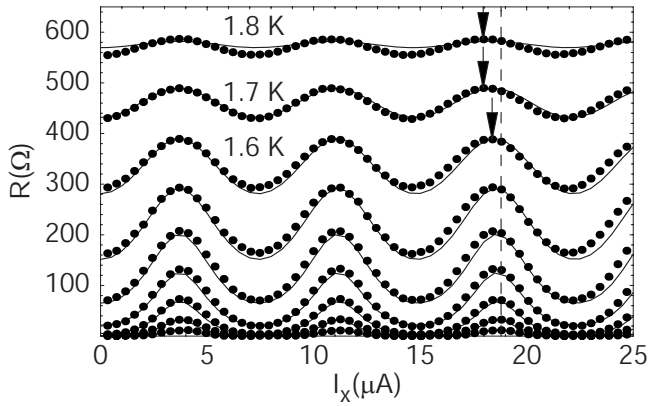

FIG. 3. Resistance vs cross-current data for sample No. 2 at temperatures ranging from 1.0 to 1.8 K in 0.1 K increments. The solid lines are fits using the same nanowire parameters as the fit for the *R-T* data in Fig. 2 and for the period vs *T* data in Fig. 4. The dashed vertical line corresponds to the position of the peak at 1 K, and is an aid to reveal the decrease in period at higher temperatures. The arrows point to peaks and show the change in the oscillation period with *T*.

rows back to its I_X=0 breadth. We show this transition in Fig. 2 for two samples, each measured at two distinct values of I_X that correspond almost exactly to the minimum and maximum observed transition breadths. The *T* dependence of the resistance follows the theory of thermally activated phase slips (TAPS),[18–20] extended to the two-wire case.[16,21] This extended theory involves a modified free-energy barrier for phase slips, which accounts for the interwire coupling mediated through the leads. In the short-wire limit, the two-wire device has the current-phase relation of a single Josephson junction with an effective critical current

$$I_{\rm eff} = \frac{\sqrt{6}}{2}\frac{\hbar}{2e}\sqrt{(I_{c1}+I_{c2})^2\cos^2\frac{\delta}{2}+(I_{c1}-I_{c2})^2\sin^2\frac{\delta}{2}},$$

tuned by the phase gain between the ends of the two nanowires δ (see Fig. 1). For the cross-current experiment, $\delta=\int_{-a}^{a}\nabla\phi\cdot d\mathbf{r}$, where ϕ is the phase of the superconducting order parameter and the integral runs between the nanowire ends via the horseshoe lead. We note that the oscillation period is independent of whether the nanowires are operating in the short-wire limit or not. Moreover, I_{c1} and I_{c2} are the critical currents for the nanowires, and are given by $I_{c1,2}=I_{c1,2}(0)[1-T/T_{c1,2}]^{3/2}$.[22,26] We obtain the device resistance *R* from the damped Josephson junction formula[23,24] [Eq. (9) of Ref. 24], where we have used the normal-state resistance R_N of the two parallel nanowires for the effective shunt resistance of the junction. Choosing δ=0 and $\delta=\pi$, we fit the lower and upper curves in Fig. 2. As shown in Fig. 3, the resistance oscillates as a function of I_X, having a period on the order of 7 μA and an amplitude that is maximal in the middle of the resistive transition. As the arrows in Fig. 3 indicate, the period of the resistance oscillation is temperature-dependent, in contrast with the case of magnetic-field-induced oscillations, which appear to be temperature independent.[16] This shows that the oscillation is not due to a magnetic field induced by the cross current.

The period of the resistance oscillation is determined by the condition that the phase gain δ be an integer multiple of 2π. For the case of a uniform cross current in a thin-film strip of width *w* and thickness *d*, $\nabla\phi=\delta/2a=(I_X/n_s)(2m/wde\hbar)$, where n_s is the superfluid density. Thus, by measuring the period of the resistance oscillation vs *T*, we obtain the superfluid density in the strip carrying the cross current, via

$$\Delta I_X(T) = \left(\frac{\pi wd}{a}\frac{\hbar e}{2m}\right)n_s = \Delta I_X(0)\frac{n_s(T)}{n_s(0)}. \quad (1)$$

The normalized period of the resistance oscillation (and hence the normalized n_s) vs *T* is shown in Fig. 4. To make the fits we have used the MB result[10]

$$n_s(T) = n_s(0)\frac{\Delta(T/T_c)}{\Delta(0)}\tanh\left[\frac{\Delta(T/T_c)}{2k_BT}\right], \quad (2)$$

where T_c is the critical temperature, $n_s(0)$ is the zero-temperature superfluid density, and $\Delta(T/T_c)$ is the universal BCS gap relation.[25] The fit to the MB formula was performed by allowing $n_s(0)$ [and hence $\Delta I_X(0)$] to be an adjustable scaling parameter. It gives better agreement than do the alternative theories, such as Gorter-Casimir and Ginzburg-Landau (Fig. 4). In fact, the fit to the MB theory can be further improved by slightly varying T_c; almost perfect fits are obtained with T_c=5.22, 5.94, and 5.56 K for samples Nos. 2, 4, and 6, respectively. Combining the obtained fitting parameters $\Delta I_X(0)$, I_{c1}, T_{c1}, I_{c2}, and T_{c2}, we produce the theoretical curves in Fig. 3 without any additional adjustable parameters.

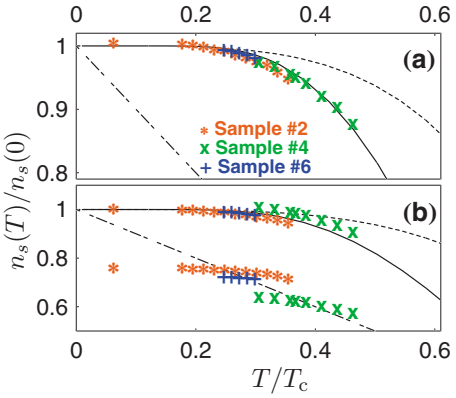

FIG. 4. (Color online) Normalized superfluid density n_s vs T/T_c. The solid line represents the Miller-Bardeen (MB) theory [Eq. (2)]; the dotted line is the Gorter-Casimir (GC) model; the dotted-dashed line is the Ginzburg-Landau (GL) formula. (a) $n_s(0)$ was chosen to optimize the MB fit, the respective scaling parameters $\Delta I_X(0)$ being 7.39, 11.70, and 7.30 μA for samples Nos. 2, 4, and 6. The values of T_c used here, 5.64, 5.72, and 5.77 K for samples Nos. 2, 4, and 6, have been measured independently. (b) The same set of data is shown, but $n_s(0)$ was chosen to optimize the GC fit (top group of points) or the GL fit (bottom group of points).

Having shown that our device is capable of sensing resistance oscillations due to phase gradients created by external supercurrents, we now turn our attention to the application of magnetic fields $\gtrsim H_{c1}$, which induce vortices in the thin-film leads, and thus create additional phase gradients. The penetration of vortices into mesoscopic samples was studied previously, using other methods (see, e.g., Refs. 27–29). All the measurements presented in the following were performed on sample No. 2. Figure 5 shows the resistance as a function of cross current at several values of applied magnetic field. At low fields, when vortices are absent, the cross-current-induced oscillations are phase shifted with respect to one another for distinct magnetic fields but with no discernible difference in the oscillation period (see the curves labeled 0

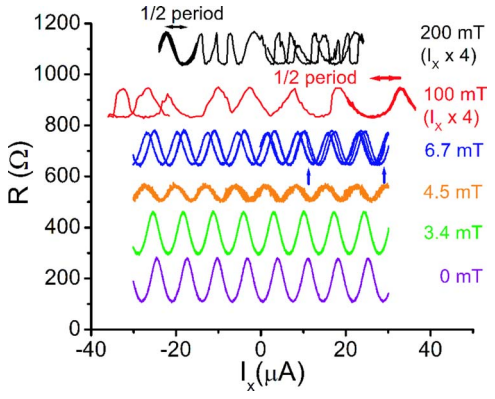

FIG. 5. (Color online) Resistance vs cross current measured at various values of the magnetic field at 1 K. For clarity, all curves, except that for 0 mT, have been offset vertically by an integer multiple of 170 Ω. The 100 and 200 mT curves have been horizontally magnified by a factor of 4, as the period became rather small at these fields. The curves show multiple random jumps at higher fields.

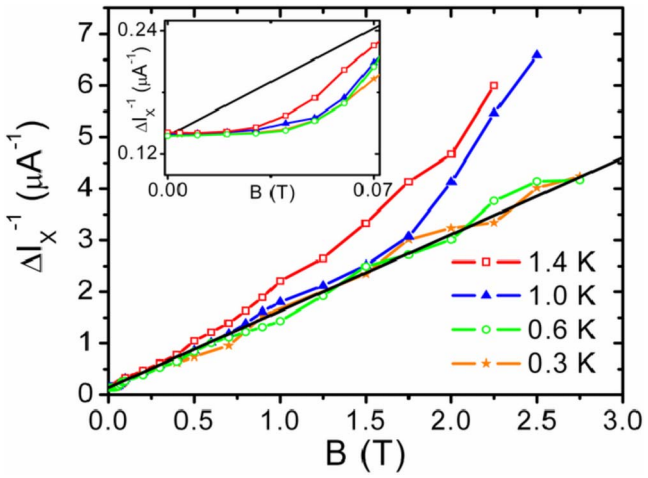

FIG. 6. (Color online) Inverse of the oscillation period vs field. The black line is from Campbell's formula with $\lambda_\perp = 46$ μm and $k = 370$ N/m^2. The inset shows the low-field data.

and 3.4 mT). This shift is due to the additional phase gradient caused by the Meissner currents associated with the applied magnetic field. At fields slightly above H_{c1} for the wider lead, it is possible to see one of two types of resistance traces. Sometimes, we observe noisy oscillations with a smaller than expected amplitude (e.g., 4.5 mT). We believe that this is due to a vortex that is rapidly wandering near one of the nanowires, i.e., a version of motional narrowing. At other times, we observe the type of oscillation as observed below H_{c1}, but with occasional jumps (6.7 mT) which become more frequent when the field is larger. At fields above H_{c1} for the cross-current carrying lead (with larger H_{c1}), the period begins to decrease, as shown by the 100 and 200 mT traces. As vortex jumps are prevalent at these fields, and our goal is to measure the period for a given vortex configuration, we determine the period by measuring it within "quiet regions" (i.e., current intervals exhibiting no jumps) as indicated by horizontal arrows for the 100 and 200 mT traces.

We have investigated the resistance oscillation period as a function of magnetic field at four temperatures by making several scans of I_X in "quiet regions," in which it was possible to observe at least one peak and one valley several times before a vortex jump occurred. At temperatures below ~700 mK, at which the device has an undetectably small zero-bias resistance, we obtained the period from large bias-current resistance measurements (i.e., beyond the linear-response regime). At each field and temperature, several measurements of the period were recorded and averaged. Smoothed curves of the inverse period, obtained via a moving average, are shown as functions of magnetic field in Fig. 6. We observe a roughly linear increase of the inverse period; compared to its zero-field value, the period at $B = 3$ T is some thirty times smaller. Such behavior is analogous to the linear dependence of the perpendicular penetration depth $\lambda_\perp$ on applied magnetic field (in the regime in which the vortex density is proportional to the field), i.e., the Campbell formula,[12–14] adapted for thin films: $\lambda_{C,\perp} = \{\lambda^2 + [\Phi_0 B/\mu_0 k(T)]\}/d$. Here, $k(T)$ is the vortex pinning force constant (i.e., the Labusch parameter[15]). In the

present setting, the phase fields from the vortices, displaced due to I_X, enhance the phase gradients created by the cross current, resulting in a period for resistance oscillations that shortens with B. We can therefore tie the Campbell prediction to the measured period by assuming the London relation $n_s = m/\mu_0 e^2 d\lambda_{C,\perp}$. From this and Eq. (1), we expect that the inverse period should increase linearly with magnetic field for our thin-film leads $(\Delta I_X)^{-1} = (2a/wd)\{\mu_0\lambda^2/\Phi_0 + [B/k(T)]\}$. We estimate that $k \approx 370\ \mathrm{N/m^2}$; other materials have yielded, e.g., $>100\ \mathrm{N/m^2}$ (Ref. 12) and $\sim 10^5\ \mathrm{N/m^2}$.[30] Furthermore, the inferred value of $\lambda_\perp(B=0)$ is consistent with an estimate made using bulk penetration-depth and film-thickness data.[31] As Fig. 6 shows, the inverse period does indeed increase linearly, except at higher temperatures and fields. In those regimes, intervortex interactions become important, and hence, k can be effectively reduced. At high temperatures, vortices explore a larger area and are less sharply pinned. For fields below $H_{c1} \sim 0.02$ T, no vortices exist in the horseshoe lead, and the period does not depend on the field. The deviation from linear field dependence observed slightly above H_{c1} (Fig. 6 inset) arises because in this regime the vortex density grows sublinearly with the field.

We conclude by remarking that our N-SQUID gradiometer can be used not only to measure the local superfluid density, e.g., in connection with the fate of the Josephson effect in ultrathin film systems,[32] but also to shed light on settings in which local fluctuations of the superfluid density have been predicted, such as highly disordered s-wave 2D superconductors[33] and superconductors having magnetic impurities.[34]

This work was supported by DOE Grants No. DEFG02-07ER46453 and No. DEFG02-91ER45439 and by NSF DMR Grant No. 0134770. D.S.H. and A.B. acknowledge the access to the fabrication facilities at the Frederick Seitz Materials Research Laboratory. We thank Russell W. Giannetta for helping to identify the connection with the Cambell law and Matthew P. A. Fisher for valuable discussions.

[1] R. C. Jaklevic, J. Lambe, A. H. Silver, and J. E. Mercereau, Phys. Rev. Lett. **12**, 159 (1964); Phys. Rev. **140**, A1628 (1965).

[2] *The SQUID Handbook*, edited by J. Clarke and A. I. Braginski (Wiley-VCH, New York, 2004), Vol. I; *The SQUID Handbook*, edited by J. Clarke and A. I. Braginski (Wiley-VCH, New York, 2006), Vol. II.

[3] See, e.g., J. Clarke, Sci. Am. **271**, 49 (1994).

[4] J. Clarke, Philos. Mag. **13**, 115 (1966).

[5] S. K. H. Lam and D. L. Tilbrook, Appl. Phys. Lett. **82**, 1078 (2003).

[6] J.-P. Cleuziou, W. Wernsdorfer, V. Bouchiat, T. Ondaruhu, and M. Monthioux, Nat. Nanotechnol. **1**, 53 (2006).

[7] W. Wernsdorfer, E. Bonet Orozco, K. Hasselbach, A. Benoit, D. Mailly, O. Kubo, H. Nakano, and B. Barbara, Phys. Rev. Lett. **79**, 4014 (1997).

[8] W. Wernsdorfer and R. Sessoli, Science **284**, 133 (1999).

[9] I. Chiorescu, Y. Nakamura, C. J. P. M. Harmans, and J. E. Mooij, Science **299**, 1869 (2003).

[10] P. B. Miller, Phys. Rev. **113**, 1209 (1959); J. Bardeen, Rev. Mod. Phys. **34**, 667 (1962).

[11] S. J. Turneaure, T. R. Lemberger, and J. M. Graybeal, Phys. Rev. Lett. **84**, 987 (2000).

[12] R. Prozorov, R. W. Giannetta, N. Kameda, T. Tamegai, J. A. Schlueter, and P. Fournier, Phys. Rev. B **67**, 184501 (2003).

[13] A. M. Campbell, J. Phys. C **2**, 1492 (1969).

[14] A. M. Campbell, J. Phys. C **4**, 3186 (1971).

[15] R. Labusch, Phys. Rev. **170**, 470 (1968).

[16] D. S. Hopkins, D. Pekker, P. M. Goldbart, and A. Bezryadin, Science **308**, 1762 (2005).

[17] D. S. Hopkins, Ph.D. thesis, University of Illinois, 2007.

[18] W. A. Little, Phys. Rev. **156**, 396 (1967).

[19] J. S. Langer and V. Ambegaokar, Phys. Rev. **164**, 498 (1967).

[20] D. E. McCumber and B. I. Halperin, Phys. Rev. B **1**, 1054 (1970).

[21] D. Pekker, A. Bezryadin, D. S. Hopkins, and P. M. Goldbart, Phys. Rev. B **72**, 104517 (2005).

[22] M. Tinkham and C. N. Lau, Appl. Phys. Lett. **80**, 2946 (2002).

[23] Y. M. Ivanchenko and L. A. Zil'berman, Zh. Eksp. Teor. Fiz. **55**, 2395 (1968).

[24] V. Ambegaokar and B. I. Halperin, Phys. Rev. Lett. **22**, 1364 (1969).

[25] For a review, see M. Tinkham, *Introduction to Superconductivity*, 2nd ed. (McGraw-Hill, New York, 1996).

[26] The T_c of the nanowires ($\sim$1.5–3 K) is smaller than that of the films ($\sim$5.5–6 K) due to disorder and electron-electron interactions. See, e.g., J. M. Graybeal, P. M. Mankiewich, R. C. Dynes, and M. R. Beasley, Phys. Rev. Lett. **59**, 2697 (1987); Y. Oreg and A. M. Finkel'stein, *ibid.* **83**, 191 (1999).

[27] G. Stan, S. B. Field, and J. M. Martinis, Phys. Rev. Lett. **92**, 097003 (2004).

[28] B. J. Baelus, A. Kanda, F. M. Peeters, Y. Ootuka, and K. Kadowaki, Phys. Rev. B **71**, 140502(R) (2005).

[29] K. Yu. Arutyunov and T. T. Hongisto, Phys. Rev. B **70**, 064514 (2004).

[30] A. A. Pesetski and T. R. Lemberger, Phys. Rev. B **62**, 11826 (2000).

[31] Using $\lambda \approx 0.55\ \mu$m [see B. L. T. Plourde, D. J. Van Harlingen, N. Saha, R. Besseling, M. B. S. Hesselberth, and P. H. Kes, Phys. Rev. B **66**, 054529 (2002)], we estimate $d \approx 6.68$ nm, compared to the sputtered thickness of 10.5 nm. We believe the discrepancy in film thickness is due to oxidation and damage caused by the FIB.

[32] M. Hermele, G. Refael, M. P. A. Fisher, and P. M. Goldbart, Nat. Phys. **1**, 117 (2005).

[33] A. Ghosal, M. Randeria, and N. Trivedi, Phys. Rev. Lett. **81**, 3940 (1998).

[34] A. Lamacraft and B. D. Simons, Phys. Rev. Lett. **85**, 4783 (2000).